Density-induced continuum resonances and quasi-bound states in the collisional-radiative equilibrium of dense plasmas

T Vallotton, O Peyrusse, D Benredjem

Density-induced continuum resonances and quasi-bound states in the collisional-radiative equilibrium of dense plasmas

T. Vallotton[1], O. Peyrusse[1], D. Benredjem[2]

[1] Université de Bordeaux-CEA-CNRS, Centre Lasers intenses et applications (CELIA), Talence, F-33405, France

[2] Laboratoire Aime Cotton, université Paris-Sud, Bâtiment 505, Campus d'Orsay, 91405 Orsay, France

E-mail: peyrusse@celia.u-bordeaux1.fr

Abstract. The aim of this work is to improve the treatment of density effects in non local thermodynamic equilibrium plasmas. The density effect on atomic structure (wavefunctions and energy levels) is modeled by an ion-sphere potential. The modification of the atomic potential, continuum lowering and appearance of resonances are shown. In particular, we show that the continuum resonances are linked to the electrons in the subshells passed into the continuum. Their presence determine the existence of partially bound configurations, which must be taken into account in the collisional-radiative model. We introduce in the set of rate equations a supplementary ionization process due to the plasma environment. This process (and its inverse) enters into the balance of all of the other process. It is equivalent to tunneling ionization where an outer electron located above the ionization threshold (and trapped by the potential barrier) crosses the barrier. As an application, we studied the influence of temperature and density on the average ionization and the ionic populations of a carbon plasma. We compared these calculations with the traditional method based on the chemical picture with continuum lowering.

PACS numbers: 52.20.Hv, 52.25.Jm

1. Introduction

Theoretical studies of atomic structure and level population distribution in hot and dense plasmas are of great interest for the understanding of many physical phenomena occuring in inertial confinement fusion plasmas, X-ray sources and astrophysical plasmas. Indeed, the knowledge of the opacity, the emissivity and the ionic charges distribution is required in plasma modelling. The density effects are usually studied in hot and dense plasmas when the local thermodynamic equilibrium (LTE) approximation is justified. However, if the density is sufficiently high to affect the atomic structure but not enough to ensure the local thermodynamic equilibrium, or if the plasma time scale is such that the bound

electron distribution does not thermalize, it is necessary to model the microscopics properties of the plasma by means of a collisional-radiative model.

In the most sophisticated LTE models (average atom or superconfiguration average models), the bound and free electrons which are treated on equal footing [1, 2, 3, 4, 5], experience a central self consistent field. The central field model assumes that each ion in the plasma is enclosed into a sphere from which the neighboring ions are excluded. The continuum density of states (DOS) obtained in these calculations exhibits resonances. Such resonances represent formerly bound states (in the low density limit) which transit into the continuum due to the density effects.

On the other hand, non-LTE (NLTE) plasmas are usually studied in the collisional-radiative framework, where the density effects are taken into account by using ad-hoc formulae for continuum lowering [6, 7]. These formulae suffer from a lack of consistency and lead to an unphysical sharp suppression of the levels. D.V. Fisher *et al* [8, 9] have proposed a more physical method based on the introduction of collectivized states in the collisional radiative model. In this method, one take into account the nearest ions to evaluate effective statistical weights. Moreover, the calculation of the rates connecting collectivized states and connecting collectivized states and free states is very difficult.

In the present work, we will rather use an approach where the resonances are taken into account by the introduction of quasi-bound configurations. For this purpose, one has to obtain free and bound electron wavefunctions which take into account the density effects. In the present study, we use the simple ion sphere model, in which the plasma is determined by its electron density, whose potential is introduced in the self-consistent calculation of the wavefunctions. A continuum density of states (DOS) is then calculated from the free wavefunctions. We then use the obtained resonances to determine quasi-bound configurations which are introduced in a collisional radiative system together with a new set of processes (tunnelling ionization and its inverse) which represents the partially bound character of these configurations.

In the following, we first present the self-consistent method used to calculate bound and free wavefunctions (Section 2). Section 3 describes the density effects on atomic structure and in Section 4, the inclusion of the density effects in a collisional-radiative model is discussed. Finally, the last section presents an application to a carbon plasma.

2. Self-consistent calculation of wavefunctions

In order to obtain the radial wavefunctions $P_{n_i l_i}(r)$ of a bound electron i in a dense plasma, we have to solve the eigenvalue equation (in the non relativistic framework for simplicity),

$$-\frac{1}{2}\frac{d^2}{dr^2}P_{n_i l_i}(r) + \left[\frac{l_i(l_i+1)}{2r^2} + V_i(r) + V_{\text{plasma}}(r)\right] P_{n_i l_i}(r) = E_i P_{n_i l_i}(r), \quad (1)$$

where the energy is in Hartree, $V_i(r)$ is the usual radial potential for the isolated ion, and $V_{\text{plasma}}(r)$ a radial potential due to the plasma. Concerning the isolated ion potential, we use the Hx scheme [10, 11]: $V_i(r) = -\frac{Z}{r} + V_{\text{D}}(r) + V_{\text{E}}(r)$, where $V_{\text{D}}(r)$ is the direct term

of the electron-electron potential and $V_{\rm E}(r)$ the exchange term. According to Cowan [11], we write

$$V_{\rm D}(r) = \sum_{j=1}^{q} w_j \int_0^\infty \frac{P_{n_j l_j}(r_1)^2}{r_>} dr_1 \tag{2}$$

$$V_{\rm E}(r) = -k_x f(r) \left(\frac{\rho'(r)}{\rho'(r) + 0.5/(n_i - l_i)}\right) \left(\frac{\rho'(r)}{\rho(r)}\right) \left(\frac{24\rho(r)}{\pi}\right)^{1/3}, \tag{3}$$

where $r_>$ =max(r, r_1), w_j is the number of electrons in the subshell j and $\rho(r) = \frac{1}{4\pi r^2}\sum_i w_i P^2_{n_i l_i}(r)$.

For $V_{\rm plasma}(r)$ we use (as mentioned previously) the ion sphere model, in which the free electron density is assumed uniform into a sphere of radius r_0. We assume that up to r_0, only bound and free electrons are present, the other ions being excluded from the sphere. Outside the ion sphere the electron and ion charge distributions compensate, i.e. the electrical neutrality is locally fulfilled for $r \geq r_0$. The radius r_0 is chosen so that for the most external bound electron, the charge of the nucleus is completely screened by the bound electrons in the lower subshells and by the free electrons into the ion sphere. Therefore (see [12]),

$$V_{\rm plasma} = \begin{cases} \frac{Z-N+1}{2r_0}(3 - \frac{r^2}{{r_0}^2}) & \text{if} \quad r < r_0 \\ \frac{Z-N+1}{r} & \text{if} \quad r > r_0 \end{cases} \tag{4}$$

where

$$r_0 = \left[\frac{3(Z-N+1)}{4\pi N_e}\right]^{\frac{1}{3}}, \tag{5}$$

Z denotes the atomic number of the ion, N the number of bound electrons and N_e the free electron density. Note that, within the ion-sphere model, it is also possible to define an average ionization depression $\Delta E = -\frac{3}{2}\,\frac{Z-N+1}{r_0}$ [13] so that the simplest way of taking account of the density effect consists in eliminating all the (unperturbed) levels such that

$$E_i > \chi_i - \Delta E, \tag{6}$$

where χ_i is the ionization potential of level i and E_i is the energy for the isolated ion. This defines the so-called "chemical picture with continuum lowering". This simple prescription will be compared below with the present approach.

In order to solve the Schrödinger equation (Eq. 1), we use a "spectral" method where the radial wavefunctions are developed on a basis of B-splines functions [14]. This method was chosen for its robustness, promptness and accuracy. For the bound states, the radial wavefunctions expansion reads

$$P_{nl}(r) = \sum_{i=2}^{Q-1} c_i B_i^k(r), \tag{7}$$

where k is the order of the B-spline, Q the total number of B-splines and c_i the coefficient of $P_{nl}(r)$ on the i^{th} B-spline. The knownledge of a radial wavefunction reduces to the

determination of all the coefficients c_i. In the previous expansion, we dropped the first and the last B-spline in order to fulfill the necessary boundary conditions, namely $P_{nl}(0) = P_{nl}(R) = 0$ with $R >> r_0$. For each l value, a generalized eigensystem has to be solved. It yields as many eigenvalues and eigenfunctions as basis functions. For the bound states (and the free states satisfying the same boundary conditions) the generalized eigensystem reads

$$\mathbf{Hc} = \varepsilon \mathbf{Sc}, \tag{8}$$

where $\mathbf{H}$ is the matrix representing the Hamiltonian in the B-spline basis, $\mathbf{S}$ the overlap matrix of the B-splines, and $\mathbf{c}$ the vector representing the coefficients c_i. We have

$$\begin{aligned} H_{ij} = & -\frac{1}{2}\int_{r_{\min}}^{r_{\max}} B_i^k(r)\frac{d^2}{dr^2}B_j^k(r)dr + \frac{l(l+1)}{2}\int_{r_{\min}}^{r_{\max}} B_i^k(r)\frac{1}{r^2}B_j^k(r)dr \\ & + \int_{r_{\min}}^{r_{\max}} B_i^k(r)V(r)B_j^k(r)dr \end{aligned} \tag{9}$$

$$S_{ij} = \int_{r_{\min}}^{r_{\max}} B_i^k(r)B_j^k(r)dr. \tag{10}$$

The radial wavefunctions for free electrons of arbitrary energy E are obtained by solving $\mathbf{H}P_{El} = E\ P_{El}$, where P_{El} is written as an expansion on the B-splines basis (see Eq.7), and where E is known *a priori*. Here, the value of the wavefunction at $r = R$ is arbitrary so there is no need to drop the last B-spline in the expansion. Instead, we set this last coefficient so that the radial wavefunction is written

$$P_{El}(r) = c_N\left[\sum_{j=2}^{N-1}\tilde{c}_j B_j^k(r) + B_N^k(r)\right], \tag{11}$$

where $\tilde{c}_j = c_j/c_N$. c_N will be obtained by the necessary normalization of the continuum wavefunctions. The system of linear equations becomes

$$\sum_{j=2}^{N-1}(H_{ij} - ES_{ij})\tilde{c}_j = ES_{iN} - H_{iN}. \tag{12}$$

Finally, the total DOS is written as $\rho(E) = \sum_l \rho_l(E)$ where ρ_l is the partial DOS, i.e.

$$\rho_l(E) = 2(2l+1)\int_0^{r_0} |P_{E,l}(r)|^2 dr. \tag{13}$$

3. Density effects on electronic structure

3.1. Modification of orbital wavefunctions, formation of resonances

The plasma potential introduces a dependence on electron density N_e for the orbitals and eigenvalues. Figure 1 shows the radial wavefunction $3d$ of the ground configuration $[\mathrm{Ar}]3d^2$ of Fe VII. One can see a noticeable increasing of the radial extension at the density $N_e = 1.1 \times 10^{24}$ cm^{-3}. For excited orbitals such as $4s$, the effect becomes

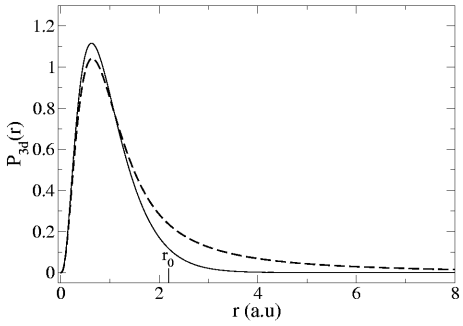

Figure 1. $3d$ radial wavefunction of the ground configuration of Fe VII at $N_e = 1.1 \times 10^{24}$ cm^{-3}. Solid line: isolated ion, dashed line: perturbed ion. r_0 is the ion sphere radius.

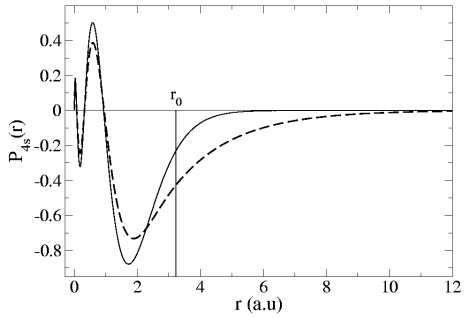

Figure 2. $4s$ radial wavefunction of the excited configuration $1s^2 2s^2 3s^2 3p^6 3d4s$ of Fe VII at $N_e = 3.3 \times 10^{23}$ cm^{-3}. Legends as in figure 1

noticeable for lower densities, as shown in figure 2. In all cases, the perturbation by the free electrons causes an extension of the wavefunction outside the ion cell. When the density is high enough the last occupied subshell moves into the continuum. For instance, in the case of the ion Fe VII in its ground configuration, the density threshold is 1.288×10^{24} cm^{-3}. More precisely, for a density above this threshold, the self consistent solution of the eigensystem does not give a negative eigenvalue for the $3d$ orbital. In other words, the $3d$ subshell has moved into the continuum. Without wavefunction for this subshell, we cannot keep the associated configuration in the rate equation system. However, this configuration does not suddenly disappear. Indeed, if we plot the potential seen by a d electron for a density just above the threshold density (see figure 3), we

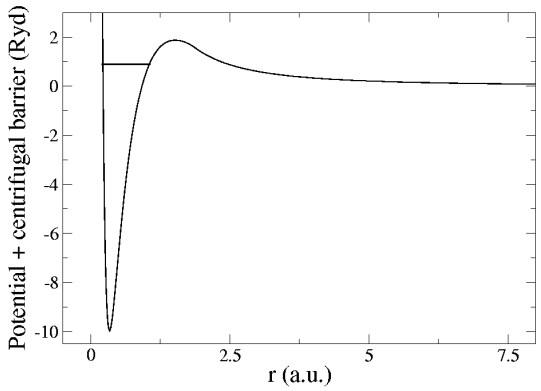

Figure 3. Potential experienced by a $3d$ electron of Fe VII for $N_e = 1.7 \times 10^{24}$ cm^{-3}. The horizontal line represents the localization of the maximum of the resonance for a $3d$ electron.

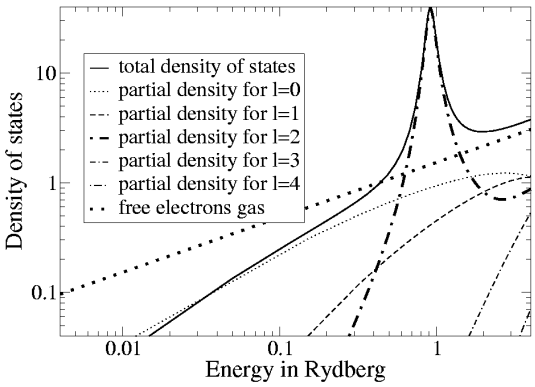

Figure 4. Total and partial DOS for the ground confiiguration of Fe VII. $N_e = 1.7 \times 10^{24}$ cm^{-3}.

observe a potential barrier. This suggests the existence of quasi-bound states with energies below this barrier. The total density of states (DOS) in the continuum of the

ground configuration of Fe VII, for an electron density of 1.7×10^{24} cm $^{-3}$, exhibits a strong resonance corresponding to these quasi-bound orbitals (see figure 4). We also plot the total and the partial DOS obtained, as well as the DOS of the free electron gas. The resonance is located at an energy of 0.9 Rydberg. At the same time, the maximum energy of the potential barrier goes up to 1.8 Rydberg (Figure 3). The free electrons states located in the resonance c orrespond to trapped electrons. The partial DOS associated with $l = 2$ largely exceeds all the partial DOS (as seen in figure 4) and the resonance clearly represents a d orbital. As the $3d$ orbital is the subshell d just passed in the continuum, it is represented by this resonance. Generally, one can say that a resonance observed in the partial DOS associated with a given l, represents the first l subshell passed into the continuum.

In order to calculate self-consistently the eigenfunctions and eigenvalues of these quasi-bound electrons, we choose to take the localized part of the free wavefunctions obtained at the maximum of the resonance, as the quasi-bound orbitals. In other words, we only consider the bound part of the wavefunction for the resonant electrons. This allows us to define partially bound configurations in the collisional-radiative system and to calculate their configuration-average energies similarly to the bound configurations. The quasi-ionized (resonant) subshells are then treated similarly to bound subshells. In figure 5, we show the free wavefunction p of the $3d4p$ configuration in Fe VII calculated for an energy located at the maximum of the resonance and for $N_e = 6.7 \times 10^{23}\text{cm}^{-3}$. As expected, the radial wavefunction behaves like a bound wavefunction for small values of r, and like a free oscillating wavefunction for large r values. The bound part of the orbital is associated with the wavefunction located in the small r region. This bound part can be obtained by connecting continuously the calculated wavefunction with an exponentially decreasing function outside the ionic sphere. Such a procedure (which must also preserves the right number of nodes) is illustrated in Fig. 5 (solid line). By doing so, we are able to obtain localized wavefunctions (renormalized in the ion sphere) for the quasi-bound electrons. This will allow us to consider these electrons in configuration-average energy calculations.

3.2. Configuration-average energies and quasi-bound configurations

Following Cowan [11], the configuration-average energy E_C^{ion} of a configuration $(n_\alpha l_\alpha)^{w_\alpha}(n_\beta l_\beta)^{w_\beta}...$, where w is the population of the nl subshells reads

$$E_C^{\text{ion}} = \sum_{\alpha=1}^{q} w_\alpha \left[E_k^\alpha + E_n^\alpha + \frac{1}{2}(w_\alpha - 1)E^{\alpha\alpha} + \frac{1}{2}\sum_{\beta\neq\alpha}^{q} w_\beta E^{\alpha\beta} \right], \tag{14}$$

where the sum runs over the occupied subshells in the configuration, E_k^α is the kinetic energy, E_n^α the electron-nucleus interaction energy, and $E^{\alpha\alpha}$ the electron-electron interaction energy. The radial wavefunction involved in Eq.13 must account for the density effects. Furthermore, the interaction of the ion with the plasma gives an energy

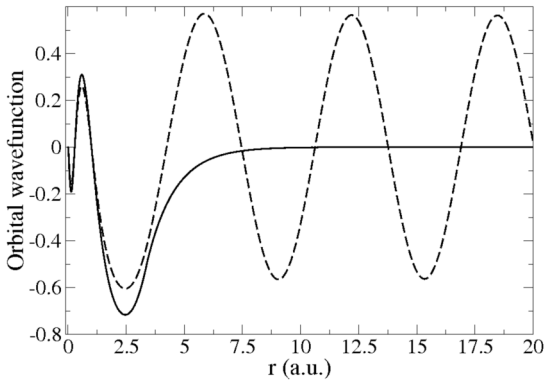

Figure 5. Radial wavefunction of Fe VII in the $3d4p$ configuration at $N_e = 6.7 \times 10^{23}\mathrm{cm}^{-3}$. Solid line: localized; dashed line: non localized.

E_C^{plasma} which is expressed as

$$E_C^{\mathrm{plasma}} = \sum_{\alpha=1}^{q} w_\alpha \int_0^\infty P_i(r) V_{\mathrm{plasma}}(r) P_i(r) dr. \tag{15}$$

The configuration-average energy of a configuration in a dense plasma is then

$$E_C = E_C^{\mathrm{ion}} + E_C^{\mathrm{plasma}}. \tag{16}$$

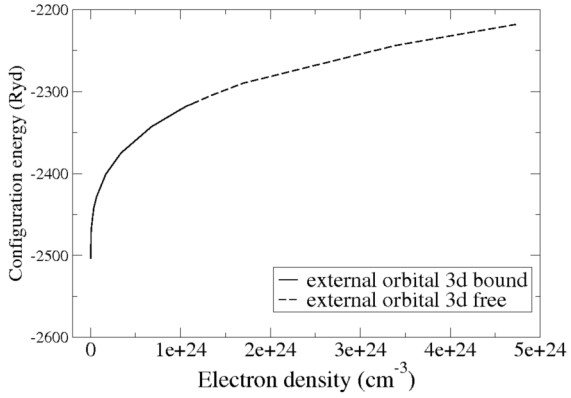

Figure 6. configuration-average energy of [Ar]$3d^2$ in Fe VII, as a function of the electron density.

It is worth stressing that E_C^{ion} and E_C^{plasma} have to be calculated even for configurations having a quasi bound orbital which exists only as a resonance in the DOS. So, as mentioned above, we consider the wavefunction at the maximum of the resonance, and then we extract its localized part. In Fig.6, we show the configuration-average energy of the ground configuration of Fe VII as a function of the electron

density. The solid line corresponds to a fully bound configuration while the dotted line corresponds to a quasi-bound part where the $3d$ orbital lies into the continuum.

We note that for increasing densities the configuration-average energy varies as $a + b\ N_e^{1/3}$ i.e. similarly to the binding energy of atomic orbitals in the ion-sphere model. It is important to note that there is no discontinuity between the two parts of the configuration-average energy.

4. Density modified energies and rates in the collisional radiative model

4.1. Variation of the configuration-average energies

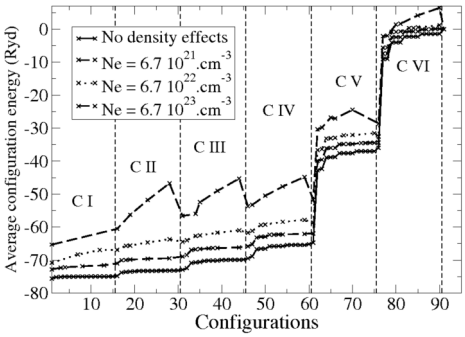

Figure 7. Configuration-average energy of carbon ion. Each cross represents a specific configuration

Our approach is now applied to a large set of configurations in various ions stages. Figure 7 shows configuration-average energies of carbon ions for various plasma densities. The bottom curve (solid line) represents the energies of C I to C VI, with 15 configurations per ion (in each charge-state, the excited configurations are obtained by promoting sequentially one electron from the ground configuration). The energies are calculated within the isolated ion approximation. The others curves are obtained for three increasing densities.

The most excited configurations (in each ion) shift into the continuum when the density increases. Among these configurations some remain quasi-bound while others are purely deleted. The latter correspond to the dilution (in the DOS) of the resonances associated with their outer orbitals. An increasing number of electronic configurations are permanently removed from the collisional radiative model when the density increases.

4.2. Density modified rates of the collisional-radiative processes

In the central field approximation used in this study and in the configuration-average context, the collisional and radiative rates depend on the configuration-average energies

and on the orbital wavefunctions. Both are affected by the density, and we have to account for the corresponding variation of the transition rates.

Concerning the radiative decay (E1) from a configuration C ($(n_1l_1)^{w_1}(n_2l_2)^{w_2}$) to a configuration C' ($(n_1l_1)^{w_1+1}(n_2l_2)^{w_2-1}$), we use the following rate (see [15]):

$$A_{CC'} = k(E_C - E_{C'})^3 \frac{w_1(g_2 - w_2)}{g_1 g_2} 2[l_1, l_2] \begin{pmatrix} l_1 & 1 & l_2 \\ 0 & 0 & 0 \end{pmatrix}^2 P_{12}^2, \tag{17}$$

where $[l_1, l_2] = \sqrt{(2l_1+1)(2l_2+1)}$, $P_{1,2} = \int_0^\infty P_{n_1l_1}(r) r P_{n_2l_2}(r) dr$, $g_i = 2(2l_i+1)$. $k = 2.677 \times 10^9$, if the energy is in Rydberg and the rate $A_{CC'}$ in s^{-1}. E_C, $E_{C'}$ and $P_{1,2}$ account for density effects.

Because quantum calculations of collisional rates are time consuming, we have used in this study semi-empirical formulae. For collisional excitation, we have used the Van-Regemorter formulae [16]:

$$K_{C'C} = N_e \times 3.2 \times 10^{-7} \left(\frac{E_H}{T_e}\right)^{3/2} f_{C \to C'} \frac{e^{-y}}{y} G(y), \tag{18}$$

where $y = \dfrac{E_C - E_{C'}}{kT_e}$ and E_H=13.6 eV. G is an average Gaunt factor for which we have taken the generalized formulation of Mewe [18], $G(y) = 0.15 + 028e^y E_1(y)$ where $E_1(y)$ is the exponential integral. The rate of the inverse process, namely the collisional deexcitation is obtained by detailed balance. For collisional ionization, the simple Lotz formulation [17] gives the following rate

$$S_{CC'} = 3 \times 10^6 N_e w_{nl} T_e^{-3/2} \frac{E_1(y)}{y}. \tag{19}$$

The rate of the inverse process, namely the 3-body recombination is obtained by detailed balance. Finally, the radiative recombination rate is given by the Seaton formula [19]:

$$R_{CC'} = 5.2 \times 10^{-14} N_e y^{1.5} e^y E_1(y) Z \; Vac(nl) \tag{20}$$

where $Vac(nl)$ is the vacancy in the nl subshell.

For these processes, the modifications induced by the density are taken into account only through the configuration-average energies.

4.3. Tunneling ionization and its inverse

We have to account for the partially bound nature of the quasi-bound configurations. In the example of figure 3, the potential clearly shows that an electron in a quasi-bound orbital can leave an ion by tunneling through the barrier. It is then necessary to introduce a new process in the rate equation system, specific to these configurations, which account for their partially bound nature.

It is well known that a discrete state interacting with continuum states of close energies leads to a decay of the discrete state. The corresponding spectrum has a lorentzian shape whose width is related to the decay rate. Moreover, this rate, called self-ionization rate or tunneling rate, is related to the width of the resonance in the partial

DOS. The width of such resonances (as discussed in the previous section) provides a transition rate to be included in the collisional-radiative equations. The rate of ionization by tunneling reads:

$$\tau_{\text{t.i.}} = 2\Gamma/\hbar \text{ (in s}^{-1}\text{)}, \tag{21}$$

where Γ is the FWHM of the resonance in the partial DOS and in $\tau_{\text{t.i.}}$, the index t.i. stands for tunneling ionization.

The inverse process of capture of an electron inside the barrier must be also taken into account. Let us apply the microreversibility principle to the tunneling ionization process. If we consider a configuration C linked by tunneling to a configuration C' with the rate $\tau_{\text{t.i.}}$, the rate τ_{capt} of the inverse process is given by

$$P_C \tau_{\text{t.i.}} = P_{C'} \tau_{\text{capt}}, \tag{22}$$

where P_C and $P_{C'}$ are the respective LTE probabilities of existence of the two configurations. Having $P_C = \frac{g_C e^{-(E_C - \mu Q_C)/kT_e}}{\sum_C g_C e^{-(E_C - \mu Q_C)/kT_e}}$, where g_C, Q_C tare the statistical weight and the number of electrons of the configuration C respectively. μ denotes the chemical potential of the free electrons. Then, we can write the rate of electron capture through the potential barrier as

$$\tau_{\text{capt}} = \frac{g_C}{g_{C'}} e^{-(E_C - E_{C'} - \mu)/kT_e} \tau_{\text{t.i.}}. \tag{23}$$

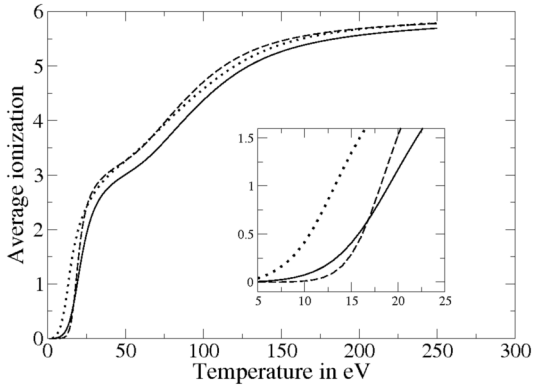

Figure 8. Average ionization of a carbon plasma as a function of temperature for $Ne = 6.7 \times 10^{22}$ cm^{-3}. Solid line: without density effects. Dashed line: with density effects (present approach). Dotted line: chemical picture with continuum lowering.

5. Average ion charge and ionic density

5.1. Carbon plasma

In this section, we focus on a carbon plasma. The advantage of such a low Z element allows us to deal with a moderate number of configurations and to neglect some

$N_e = 10^{13}$		$N_e = 10^{15}$		$N_e = 10^{17}$		$N_e = 10^{19}$	
T_e	$\overline{Z}$	T_e	$\overline{Z}$	T_e	$\overline{Z}$	T_e	$\overline{Z}$
3	1.498	3	1.705	3	1.906	3	1.094
5	2.130	5	2.174	5	2.805	5	2.245
7	2.823	7	2.865	7	3.345	7	3.066
10	3.474	10	3.519	10	3.911	10	3.813

Table 1. Average ionization of a carbon plasma as a function of Te and for different densities. The temperature is in eV and the electron density in cm^{-3}.

processes that make the calculations more complex in heavier elements. For example, autoionisation and resonant capture which both involve doubly excited configurations, can be neglected (at least when one deals with the ionization state of the plasma). We restrict the collisional radiative system to the ground configurations and one-electron excited configurations. The configuration interaction effect plays a small role and can then be ignored. The relevant configurations considered in neutral carbon are $1s^2 2s^2 2p^2$ (ground configuration), $1s^2 2s^2 2p 3s$, $1s^2 2s^2 2p 3p$, $1s^2 2s^2 2p 3d$, etc..

N_e	10^{14}	10^{15}	10^{16}	10^{17}	10^{18}	10^{19}	10^{20}	10^{21}	10^{22}	10^{23}
$\overline{Z}$	4.954	4.962	5.006	5.210	5.694	6.002	5.8926	4.941	2.912	1.373

Table 2. Average ionization of a neon plasma as a function of density for $T_e = 25eV$. The electron density is in cm^{-3}.

In Table 1 we give the average ionization $\overline{Z}$ of a carbon plasma for various temperatures and densities. Here, the plasma density effects are ignored. For comparison, we give in Table 2 the $\overline{Z}$ value in a neon plasma for an electron temperature of 25 eV. These results are in agreement with other calculations ([20, 21, 22]).

The process of tunneling ionization and its inverse as well as the energies and the modified rates discussed in previous sections are now included in the rate-equation system. In figure 8, we show the average ionization of a carbon plasma, with and without plasma density effects, which can be compared with a third curve showing the average ionization obtained with the chemical picture with continuum lowering (i.e. by eliminating unperturbed levels according to Eq. 6). The comparison of the two first curves show that the pressure ionization tends to increase $\overline{Z}$. The $\overline{Z}$ values converge for high temperatures ($\geq$ 200 eV). At moderate temperature, many partially bound configurations are populated, and the tunneling ionization and its inverse process play an important role, the effect on $\overline{Z}$ is important. For higher temperatures, the ions are highly ionized and the tunneling ionization has a small influence on the $\overline{Z}$ value. For $T_e \approx 16$ eV there is a crossing of the two curves (see the inset in Fig.8). Below this value, the density effects reduce the $\overline{Z}$ value. Comparison with the last curve (dots) shows that the simple removal of levels gives a too strong effect for $T_e < 25eV$. Furthermore, there is no crossing with the solid curve (no density effect). The crossing is clearly an

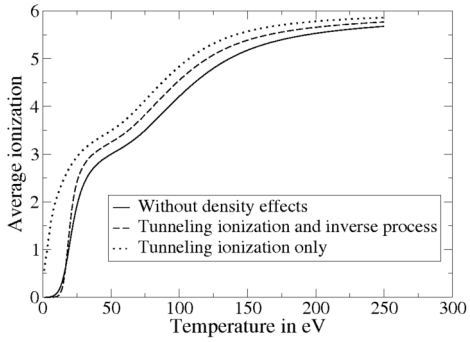

Figure 9. Average ion charge of a carbon plasma as a function of temperature, for $Ne = 6.7 \times 10^{22}$ cm^{-3}.

effect due to the two new processes introduced in our approach. It can be explained by the importance of the electron capture (over the barrier) with respect to the tunneling ionization in our rate equation system. The tunneling ionization alone always yields higher $\overline{Z}$ values in comparison with calculations performed without density effects (see Fig.9).

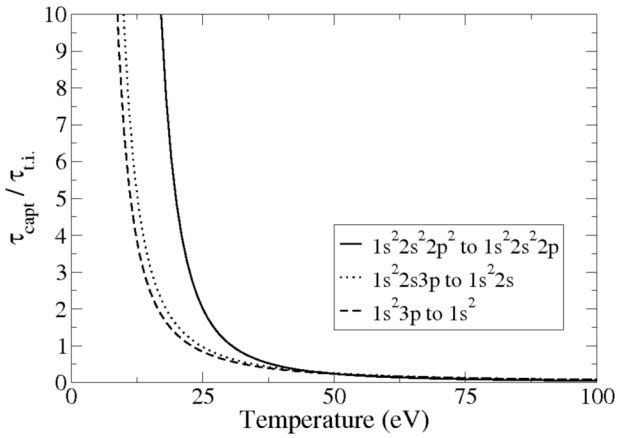

Figure 10. Ratio $\tau_{capt}/\tau_{\mathrm{t.i.}}$ for different electronic configurations as a function of Te.

Figure 10 shows the ratio $\tau_{\mathrm{capt}}/\tau_{\mathrm{t.i.}}$ for different couples of configurations, as a function of T_e. For low temperatures, this ratio is larger than 1, i.e. the process of electron capture through a barrier of potential dominates the tunneling ionization process. The ratio decreases with temperature and falls below 1 for temperatures above 50 eV.

In figure 11 we show the population densities of the various ion species. We note that the plasma density effects mainly affect the two less ionized charge states. For temperatures below 20 eV, the population of neutral carbon atoms is increased if one

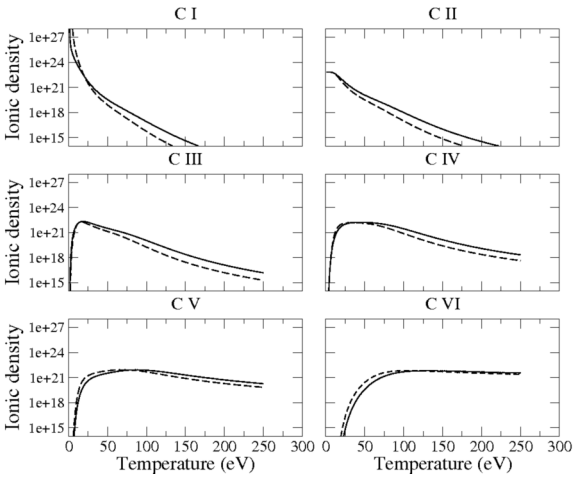

Figure 11. Population densities of carbon ions as a function of temperature (in eV). $Ne = 6.7 \times 10^{22}$ cm^{-3}. Dashed lines: with density effects, solid lines: without density effects.

takes into account the plasma density effects. For such a temperature range the electron capture dominates the tunneling ionization. In that sense, on can speak of over-barrier recombination. Above 20 eV, the population of the C I species decreases because the tunneling ionization dominates. For the ions C II, the temperature range where the population is increased by electron capture is much smaller. The population of C II increases very slightly only for $T_e < 6$ eV. For other charge states these effects are less important. There is in fact less quasi-bound configurations so the tunneling ionization plays a smaller role.

In Figure 12 we present $\overline{Z}$ as a function of temperature for other densities. If the plasma is dense enough to move all the configurations of a charge state into the continuum and to strongly broaden the associated continuum resonances, the corresponding charge state disappears. We can see that for an electron density of 6.7×10^{24}cm^{-3}, $\overline{Z}$ remains above 1 and is nearly constant for temperatures below 50 eV. Here again, we can see that the simple suppression of unperturbed levels gives a too strong ionization for $N_e > 10^{21} cm^{-3}$ and at low temperature. This is because too many levels move into the continuum (for $N_e = 6.7 \times 10^{24}$cm^{-3} all the levels of the four first charge states are lost). On the contrary, for $N_e = 6.7 \times 10^{21}$cm^{-3}, the density is too weak to affect enough levels, the obtained ionization is then nearly the same than the ionization calculated without density effects.

6. Conclusion

We have obtained orbitals for bound and free electrons in a dense plasma in the framework of a typical plasma model potential, namely the ion sphere model. In this kind of central field model, high-lying states move into the continuum as resonances, which are the trace of formerly bound electrons in the low density limit. These

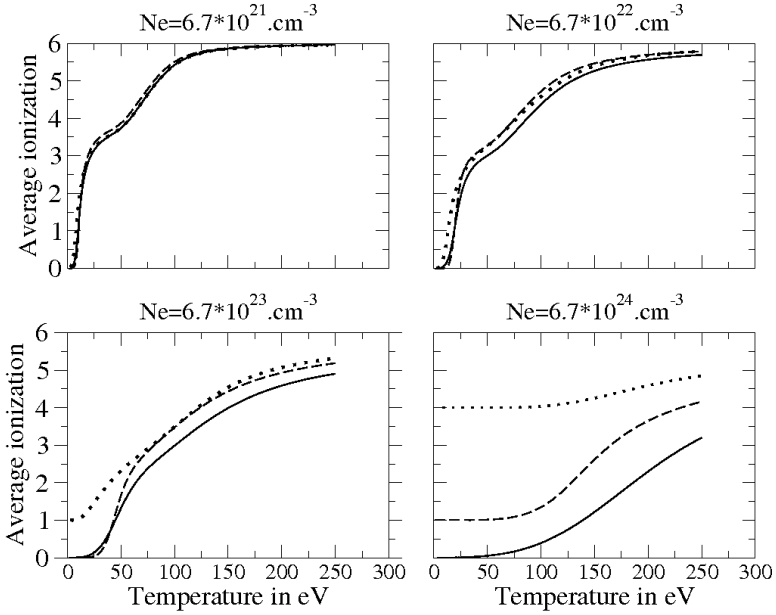

Figure 12. $\overline{Z}$ as a function of temperature and for different densities in a carbon plasma. Dashed lines: with density effects (present approach), dotted lines: chemical picture with continuum lowering, solid lines: without density effects.

resonances allow us to define quasi-bound orbitals which are included in the definition of quasi-bound configurations. These quasi-bound configurations can still be taken into account in the collisional-radiative system. We have added the tunneling ionization and its inverse process of capture. Our study uses a collisional radiative model which integrates these configurations. The obtained results differ from results obtained by mean of a simple suppression of levels. It is shown that the inclusion of the over barrier capture effect can lead to a significant recombination in some conditions.

The generalization to heavier elements would necessitate a larger number of configurations. The introduction of two-electron excited configurations is also necessary to account for processes such as autoionization and dielectronic capture. This would improve the treatment of the transition between the NLTE and LTE regimes at high densities. Furthermore, the results of this study may serve to realign more precisely, heuristic treatments of pressure ionization in collisional-radiative models.

References

[1] Liberman D A, 1979 Phys. Rev. B **20** 4981
[2] Blenski B and Ishikawa K, 1995 Phys. Rev. E. **51** 4869
[3] Wilson B, Sonnad V, Sterne P and Isaacs W 2006 J. Quant. Spectrosc. Rad. Transf. **99** 658
[4] Pain J C, Dejonghe G and Blenski T 2006 J. Quant. Spectrosc. Rad. Transf. **99** 451
[5] Piron R, Blenski T and Cichocki B 2009 High Energ. Dens. Phys. **5** 258
[6] Stewart J and Pyatt K 1966 Ap. J. **144** 1203
[7] Rouse C A 1964 Ap. J. **139** 339
[8] Fisher D V and Maron Y 2002 Eur. Phys. J. D **18** 93

[9] Fisher D V and Maron Y 2003 J. Quant. Spectrosc. Rad. Transf. **81** 147
[10] Cowan R D 1967 Phys. Rev. **163** 54
[11] Cowan R D 1981 The theory of atomic structure and spectra (Berkeley, CA: University of California Press)
[12] Massacrier G and Dubau J 1990 J. Phys. B **23** 2459
[13] More R M 1986 in *Atoms in Unusual situations*, ed. Briand J P (Plenum, New York)
[14] Peyrusse O 2006 J. Quant. Spectrosc. Rad. Transf. **99** 469
[15] Peyrusse O 1999 J. Phys. B **32** 683
[16] Van-Regemorter H 1962 Ap. J. **A132** 132
[17] Lotz W 1967 Z Phys. **206** 205
[18] Mewe R 1972 Astron. Astrophys. **20** 215
[19] Seaton M J, 1968 Advances in Atomic and Molecular Physics **4** 331
[20] Rubiano J G, Florido R, Bowen C, Lee R W and Ralchenko Yu, 2007 High Energ. Dens. Phys. **3** 225
[21] Colgan J, Fontes C J and Abdallah J R J 2006 High Energ. Dens. Phys. **2** 90
[22] Hansen S B, Fournier K B, Bauche-Arnoult C, Bauche J and Peyrusse O 2006 J. Quant. Spectrosc. Rad. Transf. **99** 272